Localized Character of $4f$ Electrons in $CeRh_x$ ($x = 2, 3$) and $CeNi_x$ ($x = 2, 5$)

Ran-Ju Jung,[1] Byung-Hee Choi,[1] S.-J. Oh,[1,*] Hyeong-Do Kim,[2] En-Jin Cho,[3] T. Iwasaki,[4] A. Sekiyama,[4] S. Imada,[4] S. Suga,[4] and J.-G. Park[5]

[1]*School of Physics & Center for Strongly Correlated Material Research, Seoul National University, Seoul 151-742, Korea*
[2]*Pohang Accelerator Laboratory, Pohang University of Science and Technology, Pohang 790-784, Korea*
[3]*Department of Physics, Chonnam National University, Kwangju 500-757, Korea*
[4]*Department of Material Physics, Osaka University, Osaka 560-8531, Japan*
[5]*Department of Physics, Sungkyunkwan University, Suwon 402-751, Korea*

(Received 1 November 2002; published 10 October 2003)

We have measured Ce $4f$ spectral weights of extremely α-like Ce transition metal intermetallic compounds $CeRh_x$ ($x = 2, 3$) and $CeNi_x$ ($x = 2, 5$) by using the *bulk-sensitive* resonant photoemission technique at the Ce $M_5(3d_{5/2} \rightarrow 4f)$ edge. High energy resolution and longer escape depth of photoemitted electron at this photon energy enabled us to distinguish the sharp Kondo resonance tails at the Fermi level, which can be well described by the Gunnarsson-Schönhammer calculation based on the Anderson impurity Hamiltonian. On the other hand, the itinerant $4f$ band description shows big discrepancies, which implies that Ce $4f$ electrons retain localized characters even in extremely α-like compounds.

DOI: 10.1103/PhysRevLett.91.157601 PACS numbers: 79.60.–i, 71.20.Eh, 71.28.+d

Ce is the first element of the $4f$ rare-earth series in the periodic table, and occupies a special place in condensed matter physics in that its $4f$ electron is believed to lie on the borderline between localization and itinerancy. Its occupied $4f$ orbital is more extended than those of heavier rare earths, and it is generally believed that an appropriate description of the interaction between the $4f$ state and the conduction bands is essential to understand the physics of Ce metal and Ce-based compounds. The famous "$\gamma - \alpha$" phase transition in Ce metal is a case in point. This isostructural transition is associated with a large volume change ($\approx$15%) and loss of magnetism, and despite intense investigations the nature of phase transition still remains controversial. The early "promotional model" [1] where one Ce $4f$ electron is presumed to go into the $5d - 6s$ conduction band in the α phase was not supported by many experiments, and two other models based on quite different starting points have emerged.

One is the Mott transition model [2], which supposes that Ce $4f$ electron is localized and nonbonding in the γ phase but becomes itinerant and forms a $4f$ band in the α phase. Recently ground state properties of Ce metal including its phase diagram have been calculated based on the self-interaction corrected local (spin) density approximation [SIC-L(S)DA] [3,4]. The other model is the Kondo volume collapse model [5,6], which proposes that $4f$ electron is localized in both γ and α phases and the phase transition is caused by the change in the conduction electron screening of the $4f$ electron. In this model the Anderson impurity Hamiltonian is used to describe both spectroscopic and thermodynamic properties [7,8], and the "$\gamma - \alpha$" phase transition was explained as being due to the variation of hybridization strength between $4f$ and conduction states [5].

These contrasting views on the nature of Ce $4f$ electron, i.e., "localized" vs "itinerant," extend to the understanding of electronic structures of Ce compounds. When Ce alloys with transition metal (TM) element to form intermetallic compounds, the hybridization between the $4f$ state and the d state of TM can be much larger than the corresponding hybridization in Ce metal [9,10]. In these so-called extremely α-like Ce-TM compounds, it was suggested that the itinerant $4f$ picture forming a narrow band is rather proper, and that this itinerant description makes correct predictions on the equilibrium lattice constant and magnetic moment in agreement with experiments for such compounds as $CeFe_2$, $CeRh_x$ ($x = 2, 3$), and $CeNi_x$ ($x = 2, 5$) [11,12]. On the other hand, physical properties of these compounds have also been analyzed within the Anderson impurity model (AIM) [13].

Photoelectron spectroscopy directly probes the electronic structure (single-particle excitation spectrum in the many-body description) of solids, and can in principle distinguish between these two contrasting pictures. Indeed for $CeRh_3$, it was once claimed that photoemission and inverse photoemission spectra are consistent with the $4f$ band picture [10,14]. However, this interpretation was challenged later [15], and many other Ce-TM compound photoemission data had been successfully interpreted within the AIM [13]. One important factor contributing to this controversy is the fact that most high-resolution photoemission experiments on Ce compounds so far have been performed with low energy photons ($h\nu \leq 150$ eV), which makes the spectra quite surface sensitive and may not represent bulk electronic structures [16,17]. Hence, to settle this controversy it is necessary to separate out the surface contributions and obtain the *bulk-sensitive* $4f$ spectra.

In this Letter, we report such study of the *bulk-sensitive* $4f$ spectral weights in extremely α-like Ce-TM intermetallic compounds $CeRh_x$ ($x = 2, 3$) and $CeNi_x$ ($x = 2, 5$), which are believed to be most likely to form itinerant $4f$ band among Ce compounds. Such bulk-sensitive high-resolution photoemission experiments were made possible recently by using high energy incident photons [18], which gives much longer escape depth of photoelectrons. In our experiments the kinetic energy of photoelectrons was ~880 eV, where the escape depth is ~17 Å and much larger than the typical surface layer thickness. From the standard formula [16], it can be estimated that the surface region contributes less than 20% to the total spectral weights and our spectra are quite bulk sensitive.

Since the photoionization cross section of Ce $4f$ electron is usually much less than those of TM d electrons, we used the resonance photoemission (RPES) technique at the Ce $3d$ edge to obtain the partial $4f$ spectral weights, where the $4f$ emission is enhanced relative to other conduction electron emissions by the process

$$3d^{10}4f^1 + \hbar\omega \rightarrow 3d^9 4f^2 \rightarrow 3d^{10}4f^0 + \text{photoelectron}.$$

Similar RPES technique at the Ce $4d$ edge has been extensively used to obtain $4f$ spectral weights of many Ce compounds [13], but in that case the small kinetic energy of photoelectrons (~120 eV) makes the spectra surface sensitive. Here we utilized RPES at the Ce $3d$ edge to obtain the bulk-sensitive spectra. One might question whether RPES gives a simple amplification of the $4f$-electron removal spectrum. We confirmed from prior experiments on other Ce compounds that the transfer function between the off-resonance and resonant spectra is close to linear, provided the incident photon energy is below the maximum of the photo-absorption peak [19,20]. This Ce $3d$-edge RPES technique has already been utilized to elucidate bulk electronic structures of several Ce compounds [21,22].

All samples of $CeRh_2$, $CeRh_3$, $CeNi_2$, and $CeNi_5$ were polycrystalline made by argon arc melting followed by annealing, and their crystal structures were checked by x-ray diffraction. The Ce $3d \rightarrow 4f$ RPES and x-ray absorption spectroscopy (XAS) measurements at the Ce $M_{4,5}$ edge were performed in the beam line BL25SU of SPring-8 in Japan. The energy resolution of the photon source around Ce $M_{4,5}$ edge was better than 80 meV [full width at half maximum (FWHM)] and the overall experimental resolution ~100 meV FWHM was obtained by SCIENTA SES200 electron analyzer. The pressure in the vacuum chamber was better than 4×10^{-10} Torr during the measurements. The data were taken at 20 K and temperature was controlled by closed-cycle He cryostat. Sample surfaces were cleaned by filing with a diamond file *in situ* and we checked the cleanliness of the surface by monitoring O $1s$ level. The Fermi level (E_F) of the sample was referred to that of surface-cleaned Pd metal.

Figure 1 shows the XAS spectra of $CeNi_x$ ($x = 2, 5$) at the Ce M_5 edge corresponding to the transition $3d_{5/2} \rightarrow 4f$. The line shape of the main peak near $h\nu = 882.3$ eV is primarily determined by the multiplet structures of the $\underline{3d}f^2$ configuration, where the underline represents a hole [24]. The slight change of this line shape and the satellite structure near ~887 eV can be understood as being the effect of hybridization between the Ce $4f$ electron and the valence band within AIM [19,25]. In the inset, we show the photoemission spectra of $CeNi_5$ taken at photon energy below this edge ($h\nu = 870$ eV; off-resonance) and very close to the maximum ($h\nu =$ 881.9 eV; on-resonance). We can see the drastic change of spectral shapes due to the much enhanced Ce $4f$ emissions on-resonance. We then extract the *bulk-sensitive* $4f$ spectral weights of each compound by subtracting off-resonance data from the on-resonance data. In this process, we use the on-resonance spectra at slightly lower (~0.6 eV) incident photon energy than the M_5 maximum peak of XAS, since the spectra taken at the M_5 maximum peak position are often found to be contaminated by incoherent Auger emissions [20].

The experimental bulk-sensitive $4f$ spectral weights of $CeNi_2$ and $CeNi_5$ thus obtained are shown as dots in Fig. 2. Previously reported $4d \rightarrow 4f$ resonant photoemission data [27] were dominated by TM $3d$ emissions and Ce $4f$ spectral features could not be clearly identified. In contrast, present data clearly show the $4f$-driven peak at E_F in both Ce-Ni compounds. To determine whether the localized or itinerant picture is more appropriate for these $4f$ spectral weights, we plot and compare with both the Ce $4f$ density-of-states (DOS) from linear muffin-tin orbital calculations with LDA (dashed line), and the Gunnarsson-Schönhammer (GS) calculation fit (thick solid line) based on the Anderson single impurity model [7]. The one-electron $4f$ DOS were taken from the published band structure calculations [10], which were convoluted with Lorentzian lifetime broadening in the usual

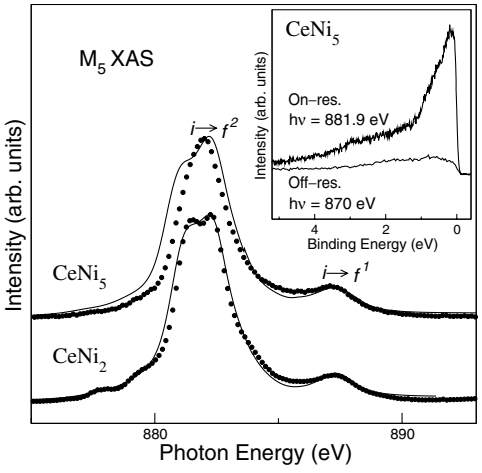

FIG. 1. The Ce M_5 XAS spectra (dots) of $CeNi_x$ ($x = 2, 5$). Solid lines are AIM fits with configuration interaction [23] using the same parameters as in Table I (see below). The inset shows off- and on-resonance photoemission data on $CeNi_5$.

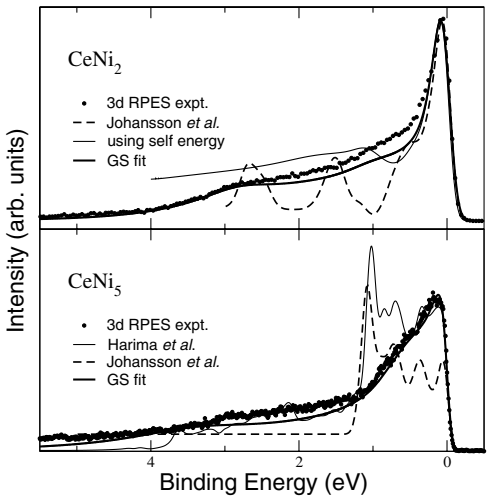

FIG. 2. Comparison between the experimental Ce $4f$ spectral weights (dots) with band structure calculations (dashed line) and with GS fits (thick solid line) for $CeNi_x$ ($x = 2, 5$). The thin solid line in the top panel is the spectral function calculated using the self-energy and the thin solid line in the bottom panel is another band calculation by Harima [26].

form of $\alpha|\omega - \omega_0|$ and the experimental resolution of 100 meV. For the GS calculations the lowest order f^0, f^1, f^2, and the second-order f^0 states were employed as basis states, and the spin-orbit splitting of the $4f$ level was included. When GS calculation is executed, it is quite essential to employ realistic $V^2(\epsilon)$ in order to fully interpret experimental spectra and fit the thermodynamic quantities [28]. Hence we used the off-resonance spectrum for the valence band shape to be hybridized with Ce $4f$ state.

From these comparisons, we can see that the GS calculations provide quite good fits for the experimental Ce $4f$ spectral weights for both $CeNi_2$ and $CeNi_5$. Their resulting parameter values are presented in Table I along with the Kondo temperature T_K, the $4f$ electron occupation number n_f, the zero-temperature magnetic susceptibility $\chi_m(0)$ deduced from these parameter values, and the experimentally measured susceptibility $\chi_m^*(0)$ [29]. We find that T_K increases and n_f becomes smaller as the Ni content is increased, which is consistent with the findings of XAS and other spectroscopic investigations [25]. This can be attributed to the shift of the Ni $3d$ valence band toward E_F at high Ni concentration [27]. We also find that the $\chi_m(0)$ value deduced from GS calculation is very close to the measured $\chi_m^*(0)$ for both Ce-Ni compounds, and the XAS data can be fit reasonably well with the same parameters as shown in Fig. 1.

TABLE I. The parameter values used for GS fitting and the resulting $4f$-level occupancy number n_f and the Kondo temperature T_K. Coulomb energy U_{ff} is set to 6.0 eV. $\chi_m(0)$'s are magnetic susceptibility at $T = 0$ predicted from GS fitting and $\chi_m^*(0)$'s are experimental values in units of 10^{-3} emu/mol.

	ε_f (eV)	Δ (meV)	T_K (K)	n_f	$\chi_m(0)$	$\chi_m^*(0)$
$CeRh_2$	1.30	95	1335	0.76	0.92	0.6
$CeRh_3$	1.20	110	1350	0.70	0.54	0.4
$CeNi_2$	1.13	89	570	0.78	1.13	0.9
$CeNi_5$	1.00	90	3300	0.69	0.62	0.7

On the other hand, the band structure calculation gives rather poor agreement with the experimental data for both compounds, especially for $CeNi_5$. The calculation does not reproduce the peak near E_F properly, and the predicted strongest peak around 1 eV from E_F is absent in the experimental data. This discrepancy is not due to the particular calculation method or misplacement of E_F, since more recent band calculation from other group (thin solid line in the bottom panel) also shows similar discrepancy [26]. For the case of $CeNi_2$, the band calculations reproduce the peak at E_F properly, but the features between 1–3 eV from E_F show appreciable discrepancy. It may be imagined that sufficiently strong self-energy correction can make this discrepancy disappear — however, when we tried to fit the spectra using the self-energy which is compatible with the Fermi-liquid theory for strongly correlated materials such as Kondo insulator [30], we found that there is still too much weight below 1 eV and spurious dip around 0.7 eV (thin solid line in the top panel).

The same phenomena happen in $CeRh_x$ ($x = 2, 3$), as can be seen in Fig. 3. In this figure, the experimental $4f$ spectral weights [31] (dots) are compared with the one-electron band structure calculation (dashed line) and the GS calculation fit (thick solid line). In both $CeRh_2$ and $CeRh_3$ the experimental data show a large peak near E_F. However, the band calculations done by two independent groups [10,26] completely miss this feature in $CeRh_3$, and predict instead a strong peak near 2 eV from E_F, which is absent in the experimental data. In the case of $CeRh_2$, the band calculation correctly predicts a peak near E_F, but

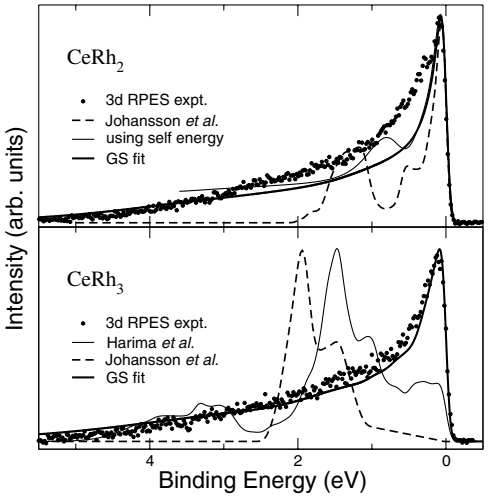

FIG. 3. The comparisons of experimentally extracted *bulk-sensitive* $4f$ weights of $CeRh_2$ and $CeRh_3$ with the one-electron band calculations and the GS fit.

again DOS below 2 eV from E_F shows substantial disagreement. The inclusion of strong self-energy correction [30] can make the agreement better (thin solid line in the top panel), but in this case the renormalization factor becomes too large and the calculated effective mass is about 4 times larger than that from specific heat measurement. In contrast, GS calculations give good general agreements in both Ce-Rh compounds, and predict reasonable magnetic susceptibility values. We list the parameter values of GS fitting for $CeRh_2$ and $CeRh_3$ in Table I along with their T_K, n_f, $\chi_m(0)$, and $\chi^*_m(0)$. We find that $\chi_m(0)$ is in good agreement with $\chi^*_m(0)$ in both Ce-Rh compounds as in the Ce-Ni case. In Figs. 2 and 3, we do not show the band calculations with self-energy corrections for $CeNi_5$ and $CeRh_3$, since they give much poorer agreements than for $CeNi_2$ and $CeRh_2$.

We can conclude from the above discussions that Anderson impurity model gives consistent description of both $4f$ spectral weights and thermodynamic properties with one set of parameter values even for the extremely α-like Ce-TM intermetallic compounds such as $CeRh_x$ ($x = 2, 3$) and $CeNi_x$ ($x = 2, 5$). In contrast, the band calculation does rather poorly in describing the photoemission spectra. This may not be surprising since the LDA is strictly valid only for the ground state, and the self-energy correction is necessary to describe single-particle excitation spectra such as photoemission. In principle, band theory with self-energy corrections and the Anderson lattice model with intersite interactions are adiabatically connected, and which approach gives a better description of electronic structures will depend on the relative strength between the intersite hopping and local electron correlation effects. In general when the Ce-Ce distance is short the intersite hybridization becomes stronger and $4f$ electrons will move closer to itinerancy. We can see this tendency in our fitting of DOS with self-energy corrections shown in Figs. 2 and 3 , where the agreement is better for $CeNi_2$ and $CeRh_2$ than for $CeNi_5$ and $CeRh_3$. However, even in these cases the electron correlation effect is fairly strong and cannot be neglected. We believe our study shows that the localized $4f$ picture is a better starting point than the itinerant band picture to understand the physical properties of these extremely α-like Ce compounds.

This work is supported by the Korean Science and Engineering Foundation through the Center for Strongly Correlated Materials Research (CSCMR) at Seoul National University. The experiments were performed under the approval of the Japan Synchrotron Radiation Research Institute. We thank Professor Harima for sending band calculation results.

*Author to whom all correspondences should be addressed.
Electronic address: sjoh@plaza.snu.ac.kr

[1] W. H. Zachariasen (unpublished) quoted in A.W. Lawson and T.Y. Tang, Phys. Rev. **76**, 301 (1949); L. Pauling, J. Am. Chem. Soc. **69**, 542 (1947).
[2] B. Johansson, Philos. Mag. **30**, 469 (1974).
[3] Z. Szotek *et al.*, Phys. Rev. Lett. **72**, 1244 (1994); A. Svane, Phys. Rev. Lett. **72**, 1248 (1994).
[4] B. Johansson *et al.*, Phys. Rev. Lett. **74**, 2335 (1995); T. Jarlborg *et al.*, Phys. Rev. B **55**, 1288 (1997).
[5] J.W. Allen and R.M. Martin, Phys. Rev. Lett. **49**, 1106 (1982); L.Z. Liu *et al.*, Phys. Rev. B **45**, 8934 (1992); J.W. Allen and L.Z. Liu, Phys. Rev. B **46**, 5047 (1992).
[6] M. Lavagna, C. Lacroix, and M. Cyrot, Phys. Lett. A **90**, 210 (1982); J. Phys. F **13**, 1007 (1983).
[7] O. Gunnarsson and K. Schönhammer, Phys. Rev. Lett. **50**, 604 (1983); Phys. Rev. B **28**, 4315 (1983).
[8] F. Patthey *et al.*, Phys. Rev. B **42**, 8864 (1990).
[9] L. Nordström *et al.*, Phys. Rev. B **44**, 10031 (1991).
[10] L. Severin and B. Johansson, Phys. Rev. B **50**, 17886 (1994).
[11] O. Eriksson *et al.*, Phys. Rev. Lett. **60**, 2523 (1988); J. Trygg *et al.*, Phys. Rev. B **50**, 4200 (1994).
[12] L. Nordström *et al.*, Phys. Rev. B **46**, 3458 (1992).
[13] J.W. Allen, S.-J. Oh, O. Gunnarsson, K. Schönhammer, M. B. Maple, M. S. Torikachvili, and I. Lindau, Adv. Phys. **35**, 275 (1986), and references therein.
[14] E. Weschke *et al.*, Phys. Rev. Lett. **69**, 1792 (1992).
[15] D. Malterre *et al.*, Phys. Rev. Lett. **73**, 2005 (1994); D. Malterre *et al.*, Adv. Phys. **45**, 299 (1996).
[16] Stefan Hüfner, *Photoelectron Spectroscopy* (Springer-Verlag, Berlin, 1995), p. 8.
[17] L. Duò, Surf. Sci. Rep. **32**, 233 (1998).
[18] Y. Saitoh *et al.*, J. Synchrotron Radiat. **5**, 542 (1998).
[19] R.-J. Jung, Ph.D. thesis, Seoul National University, Korea, 2001.
[20] E.-J. Cho *et al.*, Phys. Rev. B **67**, 155107 (2003).
[21] A. Sekiyama *et al.*, Nature (London) **403**, 396 (2000); J. Phys. Soc. Jpn. **69**, 2771 (2000); Solid State Commun. **121**, 561 (2002).
[22] T. Iwasaki *et al.*, Phys. Rev. B **65**, 195109 (2002).
[23] A. Tanaka and T. Jo, J. Phys. Soc. Jpn. **61**, 2040 (1992).
[24] T. Jo and A. Kotani, Phys. Rev. B **38**, 830 (1988).
[25] J.C. Fuggle *et al.*, Phys. Rev. B **27**, 4637 (1983).
[26] H. Harima (private communications).
[27] D. Purdie *et al.*, Solid State Commun. **106**, 799 (1998).
[28] See-Hun Yang *et al.*, Phys. Rev. B **61**, R13329 (2000).
[29] For $CeRh_2$, M. Ozawa *et al.*, Physica (Amsterdam) **206B & 207B**, 267 (1995); for $CeRh_3$, T. Gambke *et al.*, *Valence Fluctuations in Solid* (North-Holland, Amsterdam, 1981), p. 447; for $CeNi_2$, J. Sakurai *et al.*, J. Magn. Magn. Mater. **52**, 205 (1985); for $CeNi_5$, D. Gignoux *et al.*, J. Phys. (Paris) **43**, 173 (1982). Whenever possible, the susceptibility of the corresponding Y or La compound was subtracted to obtain the contribution from Ce ions only.
[30] T. Saitoh *et al.*, Solid State Commun. **95**, 307 (1995).
[31] Our $3d$ RPES data on $CeRh_3$ is somewhat different from the old data [14] in that the peak at E_F is much stronger and quite narrow. This is probably due to the difference in energy resolution and the incident photon energy.